NJC

ROYAL SOCIETY OF CHEMISTRY

COMMUNICATION

View Article Online
View Journal | View Issue

Cite this: *New J. Chem.*, 2022, **46**, 4979

Received 16th December 2021,
Accepted 11th February 2022

DOI: 10.1039/d1nj05981e

rsc.li/njc

RGB-multicolor fluorescent carbon dots by changing the reaction solvent type for white light-emitting diodes†

Xiangshan Lei,[a] Dan Li,[bc] Yajun Chen,[bc] Qingdong Liu,[bc] Qifang Yan,[bc] Jiao Wang,[c] Bingyan Han, *[bc] Gaohong He [bc] and Baigang An*[a]

In this study, carbon dots with blue, green, and red full spectrum emission were successfully prepared by changing the reaction solvent type for white light-emitting diodes.

As a new type of fluorescent carbon-based nanomaterial, carbon dots (CDs) are widely used in the fields of optoelectronic devices,[1,2] bioimaging,[3,4] fluorescence sensing[5,6] and photoelectric catalysis[7,8] because of their fluorescence tunability, good photostability, low toxicity, good biocompatibility, and accessible surface modification.

Although CDs have been studied for many years, the photoluminescence (PL) mechanism is still unclear, and it is challenging to achieve wavelength modulation throughout the visible region. The mainstream PL mechanisms of CDs include the quantum size effect, intrinsic state effect, surface state effect, molecular state effect, and cross-linked enhanced emission effect.[9–11] For example, Wang *et al.* devised an acidic reagent strategy to modulate the surface electron-giving/electron-absorbing groups of materials and successfully synthesized full-color fluorescent CDs ranging from blue to red, and even white elucidated by the quantum size effect.[12] Fang *et al.* successfully synthesized fluorescent CDs from blue to red using citric acid and aminonaphthalene as raw materials. They elucidated the PL mechanism of the intrinsic state effect.[13] Ding *et al.* isolated multicolor fluorescent CDs by a one-pot hydrothermal method and silica gel column chromatography. They proposed a surface-state PL mechanism with decreasing band gap and red-shifted wavelength with a higher oxidation degree.[14] Song *et al.* synthesized CDs using citric acid and ethylenediamine and found that the presence of molecular fluorophores in CDs greatly affected the fluorescence of CDs.[15] Yang *et al.* found that carbonized polymer dots show enhanced emission when cross-linked by covalent, supramolecular, and ionic bonds and spatial interactions in restricted domains.[16]

White light-emitting diodes (WLEDs) are of great interest in the display field because of their green, low energy consumption, and long lifetime.[17–19] High-quality WLEDs with good color rendering index are urgently needed to truly reproduce the color of objects and create a healthy atmosphere. Initially, CD-based WLEDs were prepared by simply coating a blue GaN chip with yellow CDs.[20] Due to the lack of sufficient red components, blue light from the chip of these WLEDs can cause great damage to the retina.[21] The development of multicolor emitting CDs, especially red fluorescent CDs, is an integral part of preparing WLEDs. The WLED structure based on RGB triple primary colors is characterized by a wide color space, which can produce good color rendering. Therefore, synthesis of fluorescent CDs based on RGB trichromes is essential.

Herein, red-, green-, and blue-CDs (R-, G-, B-CDs) were successfully synthesized by a simple one-pot solvothermal method changing the reaction solvent type using *o*-phenylenediamine and phenylalanine as raw materials (Scheme 1). Characterization by Raman spectroscopy and X-ray photoelectron spectroscopy (XPS) showed that the graphitization increased from B-CDs to G-CDs, the energy gap decreased, and the emission wavelength was red-shifted; the increase of graphitic nitrogen from G-CDs to R-CDs gave rise to the increase of the HOMO orbital energy level and the reduction of the energy gap, which further led to the red-shift of the emission wavelength. In addition, WLEDs were successfully prepared based on RGB primary color CDs.

[a] *School of Chemical Engineering, University of Science and Technology Liaoning, 185 Qianshanzhong Road, Anshan, 114051, China. E-mail: bgan@ustl.edu.cn; Tel: +860412-5929171*

[b] *State Key Laboratory of Fine Chemicals, Dalian University of Technology, Dalian, 116023, China*

[c] *Panjin Institute of Industrial Technology, Liaoning Key Laboratory of Chemical Additive Synthesis and Separation, School of Chemical Engineering, Dalian University of Technology, Panjin, 124221, China. E-mail: byhan@dlut.edu.cn; Tel: +86427-2631820*

† Electronic supplementary information (ESI) available. See DOI: 10.1039/d1nj05981e

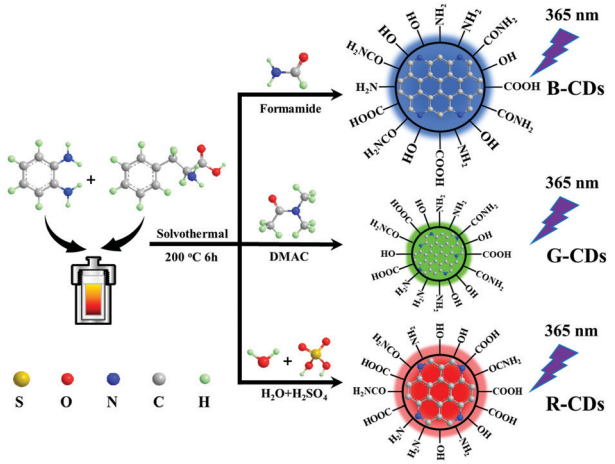

Scheme 1 Preparation of RGB-multicolor CDs by changing the reaction solvent type.

By adjusting the solvent type at 200 °C and 6 h using *o*-phenylenediamine and phenylalanine as the nitrogen and carbon sources, B-CDs were obtained by using formamide as the solvent; G-CDs were obtained by replacing the solvent with *N*,*N*-dimethylacetamide; R-CDs were synthesized in a mixture of water and concentrated sulfuric acid. The amino group and benzene ring structure in *o*-phenylenediamine facilitate the degree of conjugation of the reaction, while the carboxyl and amino groups of phenylalanine facilitate the condensation, dehydration and carbonization at high temperature to form CDs.

Fig. 1A–C show that the multicolor fluorescent CDs exhibit different colors in visible light with tunable PL from blue to red under 365 nm UV excitation. The emission centers of B-, G-, and R-CDs are 472 nm, 514 nm, and 627 nm, excited at 404 nm, 414 nm, and 561 nm, respectively. The full width at half maxima (FWHM) values of the fluorescence emission spectra from B-CDs and G-CDs to R-CDs gradually narrow from 103, to 69, to 32, respectively, because the protonated R-CDs narrow the photon transition band gap and finally trigger the red fluorescence emission on R-CDs with the narrow luminescence

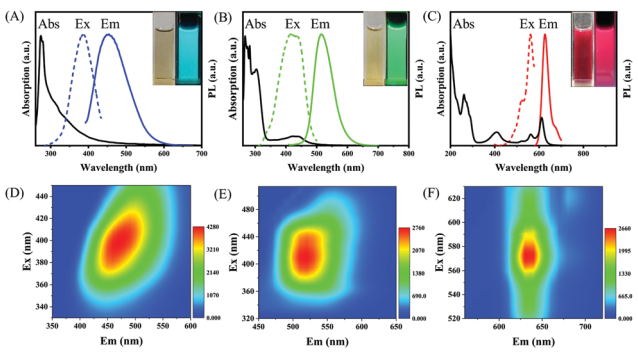

Fig. 1 Absorption and PL spectra of (A) B-CDs, (B) G-CDs, and (C) R-CDs. The insets show the corresponding photographs under daylight (left) and 365 nm UV light (right). PL emission spectra of (D) B-CDs, (E) G-CDs, and (F) R-CDs at different excitation wavelengths.

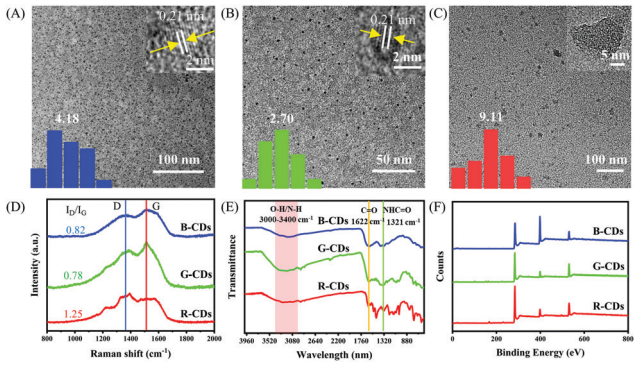

Fig. 2 TEM and HRTEM images (insets) of (A) B-CDs, (B) G-CDs, and (C) R-CDs; (D) Raman spectra of B-CDs, G-CDs, R-CDs; (E) FT-IR spectra of B-CDs, G-CDs, and R-CDs; (F) XPS spectra of B-CDs, G-CDs, and R-CDs.

band.[22] The UV absorption spectra of these three fluorescent CDs show similar absorption in the short wavelength region (200–350 nm), with absorption peaks around 270 nm and 300 nm attributed to C=C and C=N in π–π* transitions;[23] however, the visible region shows distinguishing absorption. B-CDs absorb weakly in the visible region. G-CDs and R-CDs have strong absorption peaks at 400–650 nm, which are attributed to the n–π* transitions of C=N/C=O in the aromatic sp^2 structure.[24] As shown in Fig. 1D–F and Fig. S1A–C (ESI†), compared with the excitation-independent emission properties of R-CDs, the emission properties of B-CDs and G-CDs are excitation-dependent, indicating that they contain multiple emission centers.[25] The absolute fluorescence quantum yields for B-, G-, and R-CDs are determined to be 52.34%, 65.67%, and 12.87%, respectively. As shown in Fig. S2 (ESI†), the time-resolved PL decay curves of B-, G-, and R-CDs can be fitted by a double exponential formula, and the results show that their average lifetimes are 5.82 ns, 5.71 ns and 4.94 ns, respectively.

Transmission electron microscopy (TEM) images (Fig. 2A–C) show that CDs have been successfully prepared with the average particle sizes of 4.18 nm, 2.70 nm, and 9.1 nm for B-, G-, and R-CDs, respectively. High-resolution TEM (HRTEM) shows that B-CDs and G-CDs have a lattice spacing of 0.21 nm, which is attributed to the (100) crystal plane of graphitic carbon,[26] but the lattice resolution of G-CDs is higher than that of B-CDs, indicating that the G-CDs have a higher degree of graphitization. However, the R-CDs do not have a lattice structure, indicating a lower degree of graphitization. The I_D/I_G values of B-, G-, and R-CDs were calculated by Raman spectroscopy (Fig. 2D) as 0.82, 0.78 and 1.25, respectively, which can also prove the graphitization degree of the above CDs.[27] X-Ray diffraction (XRD) patterns in Fig. S4 (ESI†) show broad peaks at around 25.5°, corresponding to the (002) crystal plane of graphite.[28]

The composition and functional groups of the CDs were investigated by Fourier transform infrared spectroscopy (FT-IR) and XPS. The FTIR shows that the B-, G-, and R-CDs all show peaks corresponding to O–H/N–H (3000–3400 cm^{-1}), C=O (1622 cm^{-1}), and NHC=O (1321 cm^{-1}) groups. The presence of NHC=O peaks indicates that the B-, G-, and R-CDs are

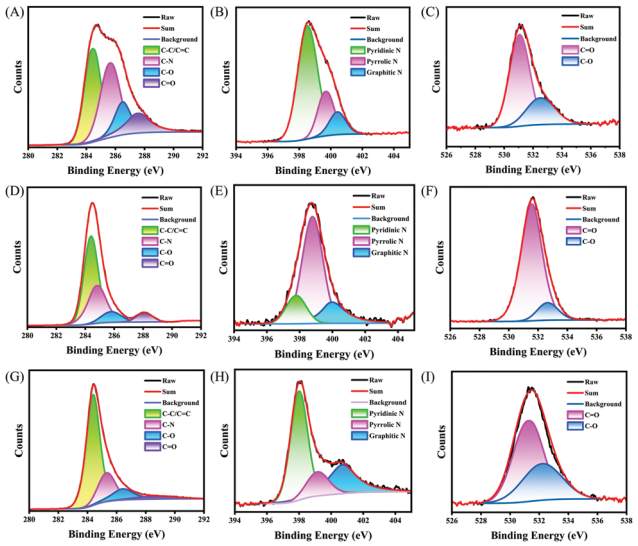

Fig. 3 High-resolution XPS C 1s spectra of (A) B-CDs, (D) G-CDs, and (G) R-CDs. High-resolution XPS N 1s spectra of (B) B-CDs, (E) G-CDs, and (H) R-CDs. High-resolution XPS O 1s spectra of (C) B-CDs, (F) G-CDs, and (I) R-CDs.

formed by dehydration of amino and carboxyl groups.[29] XPS full spectral results in Fig. 2F and Table S1 (ESI†) show that the B-, G-, and R-CDs contain three C, H, and O elements. However, the high nitrogen content of B-CDs indicates the involvement of solvent formamide in the reaction, while at the same time, the reaction solvent *N*,*N*-dimethylacetamide of G-CDs has a low reactivity with the raw materials and therefore a low nitrogen content. The high-resolution XPS (Fig. 3 and Table S2, ESI†) spectrum of C 1s deconvolution gave four main peaks of 284.4, 285.6, 286.5 and 288.6 eV, attributed to C═C/C–C, C–N, C–O, and C═O. N 1s deconvolution gave three main peaks of 398.5, 399.6, and 400.4 eV, attributed to pyridinic nitrogen, pyrrolic nitrogen and graphitic nitrogen. O 1s deconvolution gave two main peaks of 531.4 and 532.6 eV, attributed to C═O and C–O. The decrease in C═O content from B-CDs to G-CDs indicates an increase in graphitization. From G-CDs to R-CDs, the graphitic nitrogen content increases, which can reduce the HOMO–LUMO energy gap and thus redshift the emission wavelength.[30] In short, all the above characterizations clearly show that the multicolor CDs are rich in oxygen- and nitrogen-containing functional groups. The increase in graphitization from B-CDs to G-CDs brings about a red shift of fluorescence. The increase in graphitic nitrogen content from G-CDs to R-CDs further contributes to the red shift of the fluorescence.

Differences in the degree of graphitization and graphitic nitrogen lead to changes in the CDs energy levels, which affect the CDs emission wavelengths (Scheme 2). In the UV-absorption spectra (Fig. S5, ESI†), using $E_g = hc/\lambda_{Abs}$ (λ is the cut-off wavelength of UV), the energy levels of B-, G-, and R-CDs were calculated to be 3.05, 2.54, and 1.96 eV, respectively, corresponding to the red shift of the emission wavelengths. To further investigate the effects of graphitization degree and graphitic nitrogen content on the energy levels of the

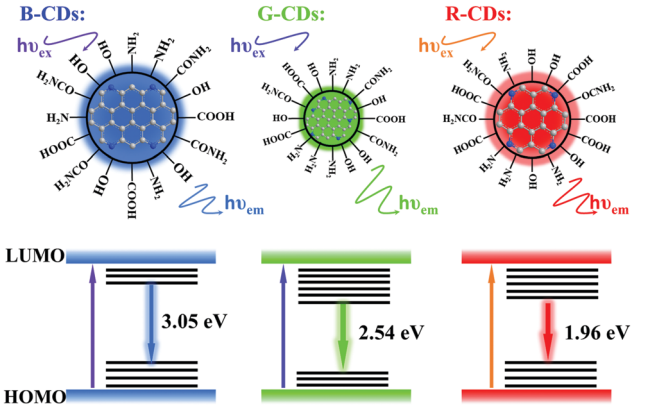

Scheme 2 Energy level diagrams of RGB-multicolor fluorescent CDs.

HOMO–LUMO orbitals, the energy level distribution was determined by UV photoelectron spectroscopy (UPS) in Fig. S6 and Table S3 (ESI†). The increase of graphitization from the B-CDs to the G-CDs gives rise to a decrease of the HOMO–LUMO energy level (from 3.05 eV → 2.54 eV), which contributes to the red shift of the fluorescence wavelength. The increase in graphitic nitrogen content from the G-CDs to R-CDs leads to an increase in the HOMO energy level, which decreases the energy gap and results in a red shift in the fluorescence wavelength. However, the solvent is the main factor that changes the fluorescence wavelength of RGB-CDs. For B-CDs, the solvent formamide has higher reactivity with the raw material compared with that of *N*,*N*-dimethylacetamide for G-CDs, which causes a high nitrogen content in the CDs, resulting in increasing the defects. So the graphitization degree is reduced, and the wavelength of G-CDs is longer compared with that of B-CDs. For the R-CDs, concentrated sulfuric acid in the solvent increases the degree of carbonization, and gives rise to an increase in the graphitic nitrogen content as well, making the emission wavelength red-shifted.

The application performance of multicolor fluorescent CDs was evaluated for WLEDs. The synthesized RGB-CDs are dispersed in an epoxy resin, and tetraethylenepentamine is used as the curing agent. WLEDs can be obtained by adjusting the ratio of blue, green and red CDs on a 365 nm UV LED chip. As presented in Fig. 4A, the fabricated WLEDs has a continuous

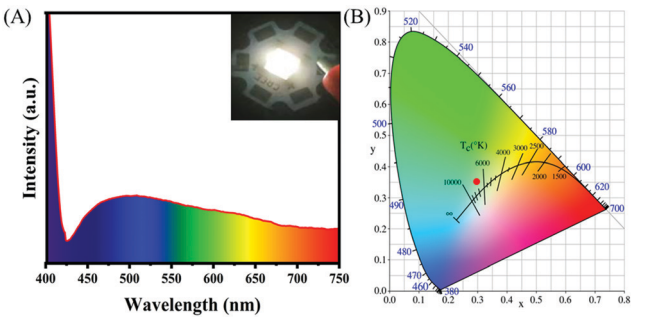

Fig. 4 (A) The emission spectrum of a WLED. (The inset shows an optical image of a WLED device.) (B) The CIE 1931 containing color coordinates of the WLED.

emission spectrum from 405 to 750 nm, which is composed of the characteristic emission of UV LED chip and RGB-CDs. The CIE coordinates of the prepared WLEDs are (0.30, 0.35), which is close to pure white light. Its color temperature is 7127 K, which is a cool white light. The Ra value reached the maximum of 86, which is higher than those reported for other CDs as shown in Table S4 (ESI†). WLEDs with high Ra value can truly reproduce the color of objects, making them promising in the display field.

Conclusions

RGB-multicolor CDs were successfully prepared by adjusting the type of reaction solvent. From the B-CDs to G-CDs, the graphitization degree increased, resulting in a decrease in energy gap and a red shift in emission wavelength. The increase of graphitic nitrogen content from the G-CDs to R-CDs leads to the increase of the HOMO orbital energy level and the decrease of the energy gap, which further gives rise to the red shift of the emission wavelength. In addition, our obtained RGB-CDs are utilized for WLEDs with an Ra value reaching 86. In the future, high performance CDs will be a considerable excellent color convertor for WLEDs.

Conflicts of interest

There are no conflicts to declare.

Acknowledgements

We gratefully appreciate the support from the Liaoning Key Laboratory of Chemical Additive Synthesis and Separation (ZJKF2103&ZJKF2011).

Notes and references

1 B. Wang, J. Yu, L. Sui, S. Zhu, Z. Tang, B. Yang and S. Lu, *Adv. Sci.*, 2020, **8**, 2001453.
2 F. Yuan, T. Yuan, L. Sui, Z. Wang, Z. Xi, Y. Li, X. Li, L. Fan, Z. Tan, A. Chen, M. Jin and S. Yang, *Nat. Commun.*, 2018, **9**, 2249–2259.
3 X. Geng, Y. Sun, Z. Li, R. Yang, Y. Zhao, Y. Guo, J. Xu, F. Li, Y. Wang, S. Lu and L. Qu, *Small*, 2019, **15**, 1901517.
4 H. Li, X. Yan, D. Kong, R. Jin, C. Sun, D. Du, Y. Lin and G. Lu, *Nanoscale Horiz.*, 2020, **5**, 218–234.
5 V. D. Dang, A. B. Ganganboina and R. A. Doong, *ACS Appl. Mater. Interfaces*, 2020, **12**, 32247–32258.
6 Y. Xu, Y. Yang, S. Lin and L. Xiao, *Anal. Chem.*, 2020, **92**, 15632–15638.
7 H. Song, M. Wu, Z. Tang, J. S. Tse, B. Yang and S. Lu, *Angew. Chem., Int. Ed.*, 2021, **60**, 7234–7244.
8 Y. Qu, X. Xu, R. Huang, W. Qi, R. Su and Z. He, *Chem. Eng. J.*, 2020, **382**, 123016.
9 S. Zhu, Y. Song, X. Zhao, J. Shao, J. Zhang and B. Yang, *Nano Res.*, 2015, **8**, 355–381.
10 L. Ai, Y. Yang, B. Wang, J. Chang, Z. Tang, B. Yang and S. Lu, *Sci. Bull.*, 2021, **66**, 839–856.
11 J. Yu, X. Yong, Z. Tang, B. Yang and S. Lu, *J. Phys. Chem. Lett.*, 2021, **12**, 7671–7687.
12 L. Wang, W. Li, L. Yin, Y. Liu, H. Guo, J. Lai, Y. Han, G. Li, M. Li, J. Zhang, R. Vajtai, P. M. Ajayan and M. Wu, *Sci. Adv.*, 2020, **6**, eabb6772.
13 F. Yuan, Z. Wang, X. Li, Y. Li, Z. Tan, L. Fan and S. Yang, *Adv. Mater.*, 2017, **29**, 1604436.
14 H. Ding, S. B. Yu, J. S. Wei and H. M. Xiong, *ACS Nano*, 2016, **10**, 484–491.
15 Y. Song, S. Zhu, S. Zhang, Y. Fu, L. Wang, X. Zhao and B. Yang, *J. Mater. Chem. C*, 2015, **3**, 5976–5984.
16 S. Tao, S. Zhu, T. Feng, C. Zheng and B. Yang, *Angew. Chem., Int. Ed.*, 2020, **59**, 9826–9840.
17 F. Yuan, P. He, Z. Xi, X. Li, Y. Li, H. Zhong, L. Fan and S. Yang, *Nano Res.*, 2019, **12**, 1669–1674.
18 B. Zhao and Z. Tan, *Adv. Sci.*, 2021, **8**, 2001977.
19 F. Yuan, Y. Wang, G. Sharma, Y. Dong, X. Zheng, P. Li, A. Johnston, G. Bappi, J. Fan, H. Kung, B. Chen, M. I. Saidaminov, K. Singh, O. Voznyy, O. M. Bakr, Z. Lu and E. H. Sargent, *Nat. Photonics*, 2019, **14**, 171–176.
20 Q. Chen, C. Wang and S. Chen, *J. Mater. Sci.*, 2012, **48**, 2352–2357.
21 M. Du, Y. Feng, D. Zhu, T. Peng, Y. Liu, Y. Wang and M. R. Bryce, *Adv. Mater.*, 2016, **28**, 5963–5968.
22 Q. Zhang, R. Wang, B. Feng, X. Zhong and K. Ostrikov, *Nat. Commun.*, 2021, **12**, 6856–6868.
23 T. Zhang, J. Zhu, Y. Zhai, H. Wang, X. Bai, B. Dong, H. Wang and H. Song, *Nanoscale*, 2017, **9**, 13042–13051.
24 S. Lu, L. Sui, J. Liu, S. Zhu, A. Chen, M. Jin and B. Yang, *Adv. Mater.*, 2017, **29**, 1603443.
25 Y. Zheng, K. Arkin, J. Hao, S. Zhang, W. Guan, L. Wang, Y. Guo and Q. Shang, *Adv. Opt. Mater.*, 2021, **9**, 2100688.
26 W. Li, Y. Liu, M. Wu, X. Feng, S. A. T. Redfern, Y. Shang, X. Yong, T. Feng, K. Wu, Z. Liu, B. Li, Z. Chen, J. S. Tse, S. Lu and B. Yang, *Adv. Mater.*, 2018, **30**, 201800676.
27 Y. Zhao, C. Ou, J. Yu, Y. Zhang, H. Song, Y. Zhai, Z. Tang and S. Lu, *ACS Appl. Mater. Interfaces*, 2021, **13**, 30098–30105.
28 S. Wei, X. Yin, H. Li, X. Du, L. Zhang, Q. Yang and R. Yang, *Chem. – Eur. J.*, 2020, **26**, 8129–8136.
29 Y. Ru, L. Sui, H. Song, X. Liu, Z. Tang, S. Q. Zang, B. Yang and S. Lu, *Angew. Chem., Int. Ed.*, 2021, **60**, 14091–14099.
30 K. Holá, M. Sudolská, S. Kalytchuk, D. Nachtigallová, A. L. Rogach, M. Otyepka and R. Zbořil, *ACS Nano*, 2017, **11**, 12402–12410.

